EXPERIMENTAL TEST OF SEMI-ACTIVE SHUNT DAMPING ON A HELICOPTER TRIM PANEL

Martin Pohl (martin.pohl@dlr.de), Thomas Haase (thomas.haase@dlr.de)
German Aerospace Center (DLR) Braunschweig, Germany

Abstract

The increased need for lightweight structures in modern aerospace transport due to lower fuel consumption and increased transport capacity reveals an acoustic challenge. Because of the high stiffness and low mass the coincidence frequencies of lightweight structures are low compared to classical aluminum structures. That is the reason for a weak transmission loss of lightweight structures made of glass or carbon fiber reinforced plastics. Therefore, passive solutions are widely investigated to increase the transmission loss of lightweight helicopter trim panels. For example, in the European GARTEUR AG 20 "Cabin internal noise: simulation and experimental methods for new solutions for internal noise reduction", two helicopter trim panels are studied which are structurally optimized for an increased TL.
In this paper the applicability of a semi-active shunt damping system to this structurally optimized helicopter trim panel is investigated experimentally. Prior to this, the semi-active shunt damping performance is studied on a classical steel plate and afterwards the damped helicopter trim panel is investigated in a transmission loss facility.
Two experiments are conducted. First of all, the trim panel is excited with a point force and the surface vibrations are measured with a laser scanning vibrometer. In the second test the trim panel is excited with a diffuse sound field. It can be seen that the negative capacitance shunt is less effective on a higher damped structure. Global vibration reductions of only $3-4\,\mathrm{dB}$ are achieved during the shaker test. Concerning the transmission loss, the results are comparable to the vibration reduction. The main reason for this is supposed to be a lower piezoelectric coupling to the sandwich panel.

1 INTRODUCTION

For ecologic sustainability and decreasing reserves of fossil energy sources, fuel efficiency is a major concern especially for aerospace vehicles such as passenger aircraft or helicopters. Therefore, lightweight structures made from carbon fiber reinforced plastics offer great potential in reducing structural mass, which results in higher payload and lower fuel consumption. But with increased stiffness, reduced wall thickness and lower density, they have the disadvantage of lower damping and coincidence frequencies compared to conventional differential metal constructions. Both aspects lead to an increased sensitivity of lightweight structures concerning vibration and noise radiation. In the same manner, the acoustic transmission loss (TL) is affected. For that reason, special noise and vibration treatment is needed to ensure passenger cabin comfort. In the European GARTEUR AG 20 "Cabin internal noise: simulation methods and experimental methods for new solutions for internal noise reduction", two helicopter trim panels are studied which are structurally optimized for an increased TL.

An additional opportunity for a further improvement of the TL is offered by active noise and vibration treatment, such as active structural acoustic control (ASAC). The drawback of active control methods is their need for complex system models and electronics as e.g. shown by Fahy and Gardonio [1]. Besides these two concepts, piezoelectric shunt damping is investigated. Hereby piezoelectric transducers are applied to a vibrating structure to convert mechanical

vibration energy into electric energy. Together with an appropriate electric shunt network connected to the electrodes of the transducer, the transducers can be used for vibration attenuation [2], [3], [4].

To investigate the potential of piezoelectric shunt damping, experimental measurements of damped panels are presented in this paper. To achieve a broadband effect, negative capacitance circuits are used therefore. First, preliminary measurements are performed at a steel panel, where a very good damping effect is demonstrated. Second the helicopter trim panel is equipped with piezoelectric transducers and shunt circuits. In this case the damping effect is much less compared to the pretests at the steel panel.

2 PIEZOELECTRIC SHUNT DAMPING

"Piezoelectric shunt damping" subsumes all concepts, where an oscillating structure is damped with applied piezoelectric actuators connected to electric shunt networks. The basic principle can be seen in Figure 1.

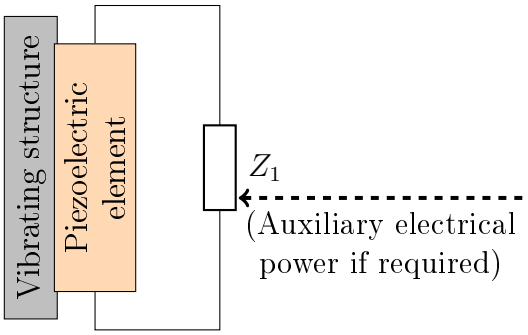

Figure 1: Working principle of piezoelectric shunt damping

The basic idea of piezoelectric shunt damping is the conversion of mechanical vibration energy from the oscillating structure into electrical energy by piezoelectric transducers. The dissipation of the converted electrical energy acts as an additional damping to the structure. Due to their relatively high piezoelectric coupling, Lead Zirconate-Titanate (PZT) ceramic transducers are commonly used in this application. In order to ensure damping, the shunt network has to fulfill two tasks. First it has to dissipate the converted vibration energy. In the easiest way, this may be achieved by using a single resistor as shunting element. In this combination, the inherent capacitance of piezoelectric transducers shown in Figure 2 would dominate the electrical behavior of the transducer. Therefore, the shunt network must be able to match the impedance of the piezoelectric transducer in a way to compensate the inherent capacitance of the transducer. By this, the energy conversion from the mechanical to the electrical system is maximized.

Several concepts for this goal are known from the literature. In order to damp a single or a few eigenfrequencies, purely passive solutions only consisting of several inductors, resistors and capacitors can be used. Such systems have been investigated in the past by Hagood and Flotow [5]. They are comparable to mechanical tuned mass vibration absorbers and use electrical resonances for damping improvement at the mechanical eigenfrequencies. An advantage is the passive character of these systems, what means, that they only consist of passive electric components with no need for an external power supply. The disadvantage lies in the narrow bandwidth, which only covers one eigenfrequency. By adding passive filters, also a damping of more than one eigenfrequency is possible as shown e.g. by Hollkmap [6] or Behrens [7]. However, these concepts are only feasible for a few modes due to the need of an increasing number of electric components per mode.

Because of the broadband performance, the negative capacitance shunt is well suited for systems with multiple modes and varying eigenfrequencies, such as panel structures under broadband excitation. This was demonstrated using a beam structure by Behrens et. al. [2] and Park et. al. [8], who achieved a remarkable damping effect for

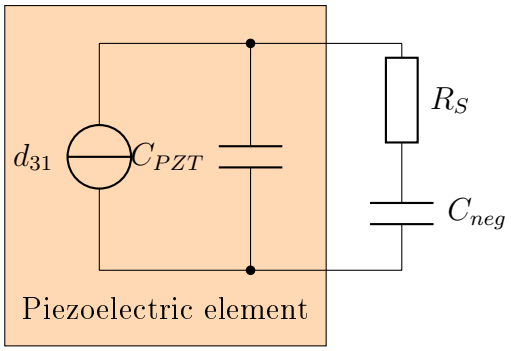

Figure 2: Working principle of negative capacitance shunt

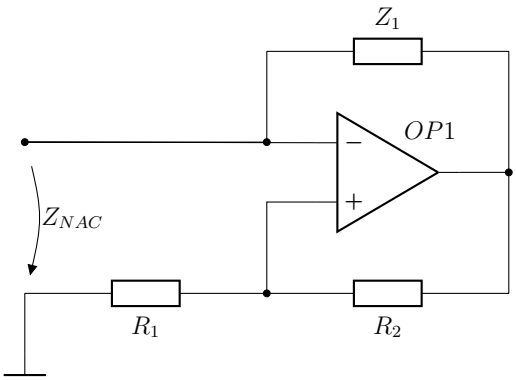

Figure 3: Negative admittance converter (NAC) (from [10])

multiple eigenfrequencies of a clamped beam.

The basic working principle of the negative capacitance shunt itself is shown in Figure 2. In this setup, the impedance matching between the structure and the electrical system is achieved by compensating the inherent capacitance of the piezoelectric element C_{PZT}, which is the main drawback for an efficient energy transfer as mentioned above. Therefore an external capacitance C_{neg} with negative sign is used. As expected, the maximum effect will be realized if $C_{neg}/C_{PZT} \rightarrow -1$. The damping itself is caused by the shunting resistor R_S in series to the negative capacitance, where the vibration energy is dissipated. Figure 2 shows the series configuration, which is subject for this paper. Of course, also a parallel configuration of R_S and C_{neg} is possible with a generally comparable behavior. A deeper insight into serial and parallel negative capacitance networks is given by Park [9].

In fact, capacitances with a negative sign cannot be realized by the exclusive use of passive electronic components. The usual way for this is to use so-called negative impedance (NIC) or negative admittance converters (NAC). These systems are based on operational amplifiers (OpAmps) and passive components as shown in Figure 3 for a NAC to invert the sign of any impedance. In the case of a NIC, the inputs of the OpAmp are reversed.

According to Philbrick [10], the impedance of the NIC and NAC can be calculated as shown in equation 1. Obviously, if a capacitor is used in the NIC or NAC circuit, a negative capacitance results.

$$Z_{NAC} = -Z_1 \cdot \frac{R_1}{R_2} \tag{1}$$

Remarkable amplitude reductions at the eigenfrequencies have been demonstrated by Pohl and Rose [11] with up to 20 dB in vibration amplitude. Therefore it is of interest, if the acoustic parameters of sandwich helicopter trim panels can be improved by negative capacitance shunting. To investigate this, preliminary experiments on a steel panel are presented first. Second, a glass fiber sandwich is equipped with the same amount of piezoelectric transducers than the steel panel to measure the effect of shunt damping. Finally, the obtained results are discussed.

3 PRELIMINARY TESTS AT STEEL PANEL

As presented in [11], negative capacitance shunting offers a remarkable damping potential. There, in fact, a relatively small steel disc was investigated, which had nearly completely been covered with piezoelectric transducers. Due to the high density of PZT and the

required mass for the electrical circuits, the total amount and the covered surface fraction of the panel must be smaller for airborne structures. Therefore pretests on a steel panel are intended to investigate the effectiveness of a smaller fraction of transducers on the panel. For these measurements, a steel panel of $800 \times 600 \times 2\,\text{mm}$ size is used, which is fixed in its corners by bolts. A sketch of this panel is provided in Figure 4. A shaker is used to excite the panel at the shown location of the excitation force F_{exc} in Figure 4.

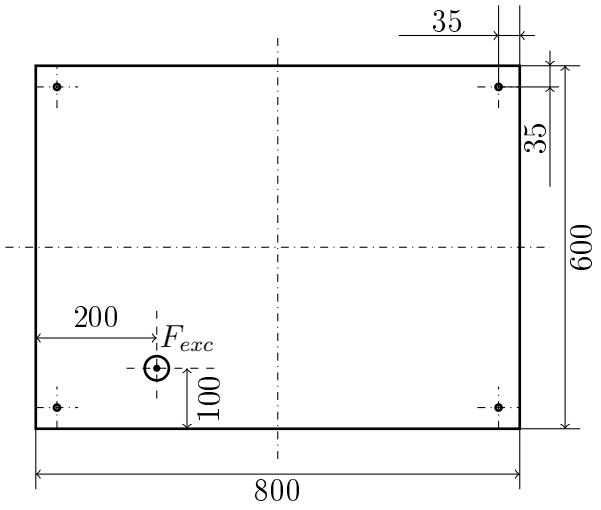

Figure 4: Dimensions of steel test panel

In order to damp the oscillations of the panel, 10 locations of piezoelectric patch transducers have been optimized for minimum vibration amplitude with a numerical model using a genetic algorithm. In this case, any location is connected to an individual negative capacitance circuit to avoid current flows between different locations. More information about the used models is given in [12]. Based on the optimization, the locations of the transducers given in Figure 5 are obtained and a test panel is built. Therefore, four DuraAct™P-876.A12 transducers [13] of $50 \times 30\,\text{mm}$ are used at each location, electrically connected in parallel to one individual shunt circuit.

As mentioned, serial negative capacitance circuits are used for the experiments. Figure 6 shows the corresponding schematic for one circuit with all components. The marked area in the dashed line covers the NAC circuit, which produces a capacitance with negative sign.

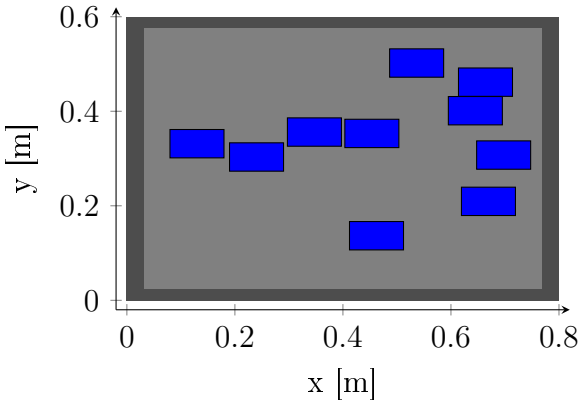

Figure 5: Transducer configuration on panel for vibration reduction

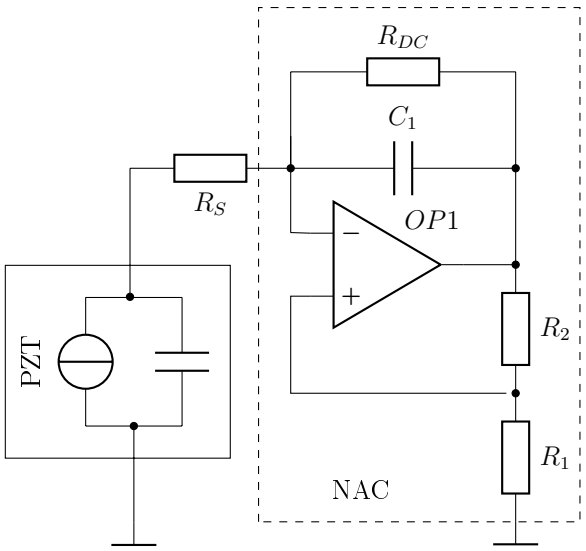

Figure 6: Serial negative capacitance circuit used in the experiments

In Table 1 the values of the used components are listed. There, the values of the inherent capacitances of the PZT transducers can only be given approximately due to variances caused by production. In fact, this does not affect the function of the circuit, because the ratio of the negative capacitance referred to the inherent capacitance C_{neg}/C_{PZT} is tuned manually by adjusting the resistor R_1 to the right value, where the circuit is at the edge of its electrical stability, where best

damping is achieved [4], [12]. By this, values of $C_{neg}/C_{PZT} = -1.06...-1.03$ were achieved. As operational amplifier, OPA445 types [14] are used with a supply voltage of $\pm 45\,\mathrm{V}$.

Table 1: Values of used negative capacitance components

component	value
R_2	$100\,\mathrm{k\Omega}$
R_S	$100\,\Omega$
R_{DC}	$10\,\mathrm{M\Omega}$
C_1	$570\,\mathrm{nF}$
C_{PZT}	$\approx 360\,\mathrm{nF}$

Due to the low amount of components, multiple circuits can be arranged easily. For the intended experiments, a printed circuit board (PCB) containing 20 individual circuits, has been designed and built as shown in Figure 7. The blue box with the brass colored screw is a potentiometer, which represents R_1 for easy and precise adjustment.

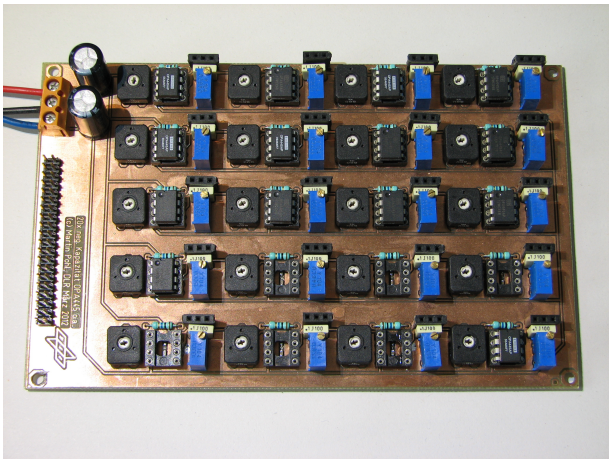

Figure 7: PCB with 20 negative capacitance shunt circuits

With the explained test settings, the vibration amplitude of the steel panel has been measured at 1270 different locations equally distributed on the panel using a Polytec PSV-400 laser scanning vibrometer. To compare the vibration amplitude of the panel with open electrodes at the transducers and with connected negative capacitance circuits, Figure 8 shows the frequency response functions (FRF) of the mean vibration amplitude referred to the excitation force. By using the FRF, the effect of spatial and time deviations in the excitation amplitude is canceled.

As can be seen in Figure 8, the modal density of the steel panel is high up to a frequency of 2 kHz, resulting in a variety of resonance peaks in the undamped transfer function with open electrodes at the transducer. Second, the negative capacitance damping effect is present over the whole measured frequency range, where the best amplitude reductions occur in a frequency range from $\approx 300\,\mathrm{Hz}$ to $\approx 1200\,\mathrm{Hz}$ with values of up to 30 dB for specific resonances. Above and below these frequencies, the effect decreases. In general, it can be stated that the expectations of a remarkable damping effect over a wide frequency range is equally fulfilled for a wider panel with a lower coverage of piezoelectric transducers compared to [11].

For a better visualization of the broadband effect, the spectra shown in Figure 8 are summed to 3rd octave bands. Figure 9 shows the corresponding graphs for the panel with and without negative capacitance circuits. There it can be seen, that a remarkable amplitude reduction of partially more than 10 dB is achieved in 3rd octave bands. Only for very low frequencies below 100 Hz, the effect vanishes. Even at the high end of the measured frequency range, an amplitude reduction of $\approx 7\,\mathrm{dB}$ is possible, which corresponds to less than half of the initial vibration amplitude.

Concluding the pretests on the steel panel, the expectations of negative capacitance shunting can be seen as fulfilled in terms of amplitude reduction and wide band damping performance. Over the whole measured frequency range, an amplitude reduction could be obtained and a continued damping effect is probable above this frequency, although with decreasing amplitude. Therefore negative capacitance shunting appears promising and

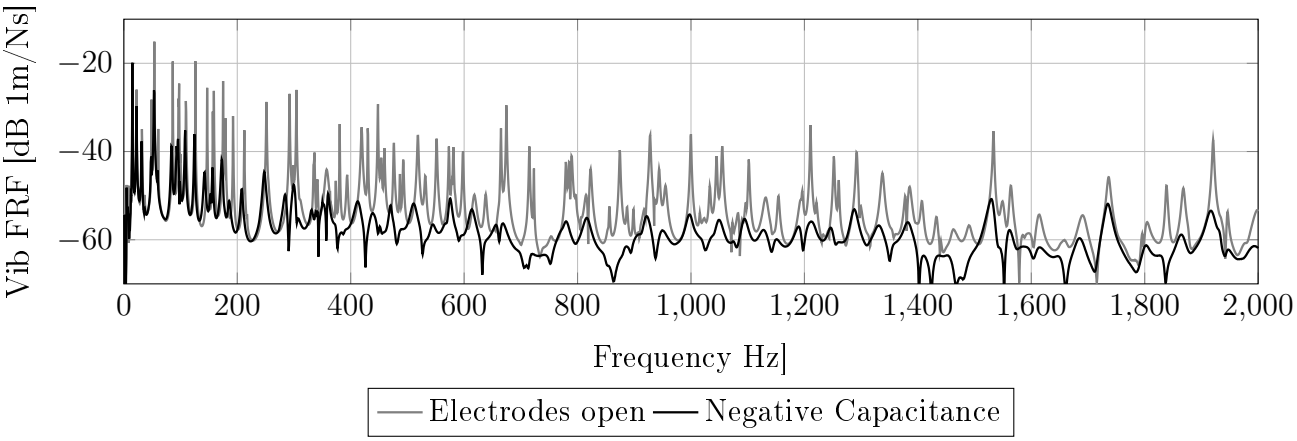

Figure 8: Vibration FRF of steel panel with and without negative capacitance circuits

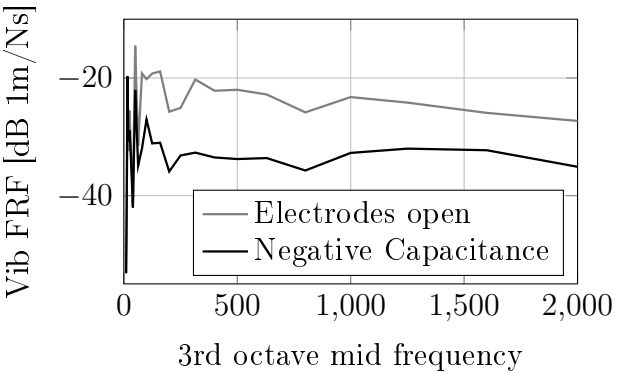

Figure 9: 3rd octave Vibration FRF with and without negative capacitance circuits

a further investigation on the behavior of such systems on glass fiber sandwich panels appears worthwhile.

4 EXPERIMENTAL INVESTIGATION OF SANDWICH TRIM PANEL

In the following section, negative capacitance shunting is investigated for a sandwich panel. The test specimen has a size of 900×900 mm at the outer edges and is by that approximately one and a half times bigger than the steel panel used in the tests before. The sandwich itself has a thickness of 11.7 mm and comprises a foam core with glass and aramid shell laminates as illustrated in Figure 10. Additionally, the material parameters of the panel components are listed in Table 2.

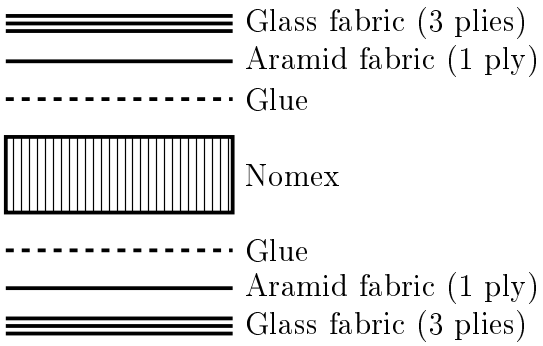

Figure 10: Laminate layup of sandwich panel

A sketch of the panel with its dimensions is given in Figure 11. The dashed line at the edge of the panel indicates the the clamping zone, where the panel is fixed in the transmission test opening.

With this panel, two characteristics will be measured. First the vibration behavior is investigated in the same way like the steel panel. A shaker is used to excite the panel at the position shown in Figure 11 and the vibration response is again measured over the whole surface using the scanning vibrometer.

Second, the TL will be investigated, since this is the desired application for such helicopter trim panels. Therefore the panel is mounted in the test opening in the acoustic transmis-

Table 2: Material parameters of sandwich panel

Parameter / Layer	Glass fabric	Aramid fabric	Glue	Nomex
ρ $[kg/m^3]$	1600	1300	1000	32
t [mm]	0.22	0.186	0.2	9.5
E_{xx} [MPa]	16200	27500	1680	$\rightarrow 0$
E_{yy} [MPa]	16200	27500	1680	$\rightarrow 0$
E_{zz} [MPa]				80
ν	0.15	0.09	0.4	/
G_{yz} [MPa]	2750	2000	600	13
G_{xz} [MPa]	2750	2000	600	23
G_{xy} [MPa]	2750	2000	600	/

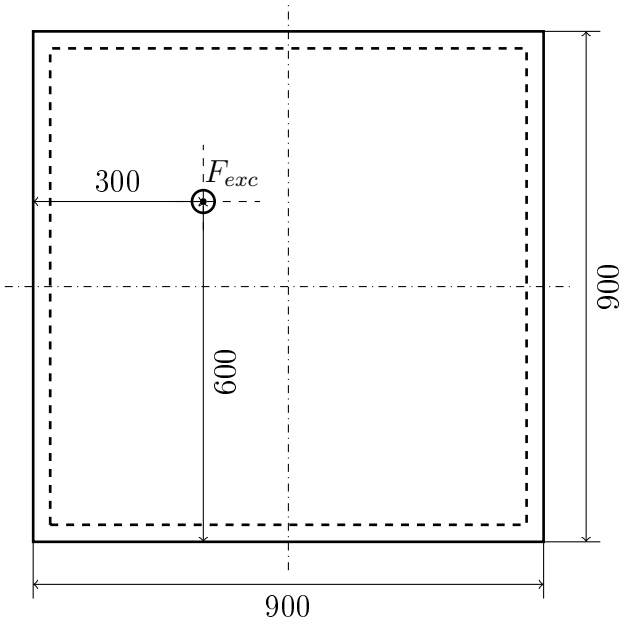

Figure 11: Dimensions of sandwich test panel

sion loss test facility at DLR in Braunschweig. To measure TL, an acoustic excitation is implemented in a reverberant room on one side of the test specimen. On the other side, a free-field room is used to obtain the radiated sound power by scanning the surface with a sound intensity probe. To provide an impression of the TL measurement, a photo of the panel mounted to the test opening seen from the excitation side is given in Figure 12.

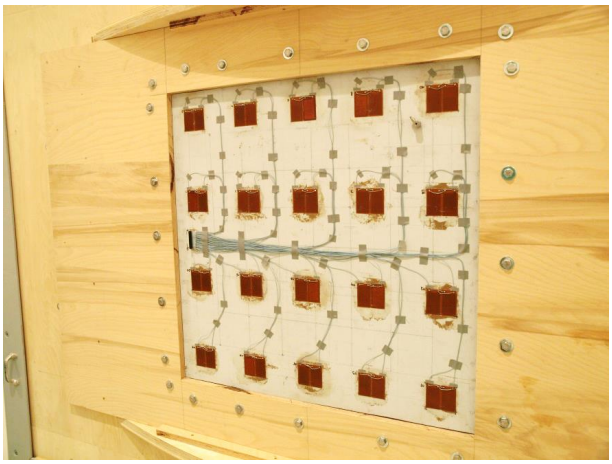

Figure 12: Panel mounted in acoustic transmission test facility

In Figure 12 the piezoelectric transducers are already applied and can be seen as brownish rectangular areas on the surface of the panel. In contradiction to the steel panel, 20 different locations with two patches in parallel have been used in a regular distribution. By that, the total transducer surface is exactly the same as the one used at the steel panel.

First the influence of the piezoelectric transducers is investigated. Because they are adding mass and stiffness to the sandwich panel, changes in the vibration response are expectable. Therefore Figure 13 shows the vibration FRFs for the panel before and after the application of the transducers. In total, a transducer mass of $40 \times 3.5\,\mathrm{g} = 140\,\mathrm{g}$ has been added to the panel.

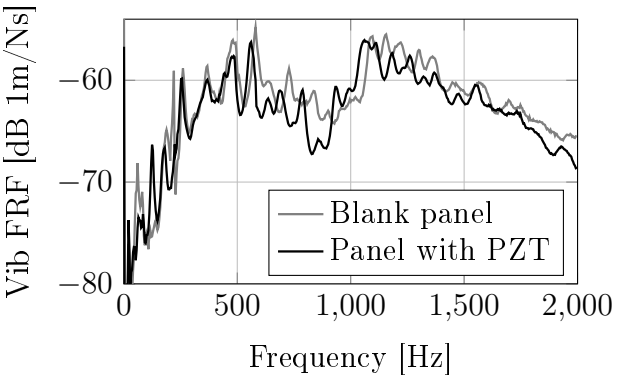

Figure 13: Vibration FRF of blank panel and with 40 applied PZT transducers

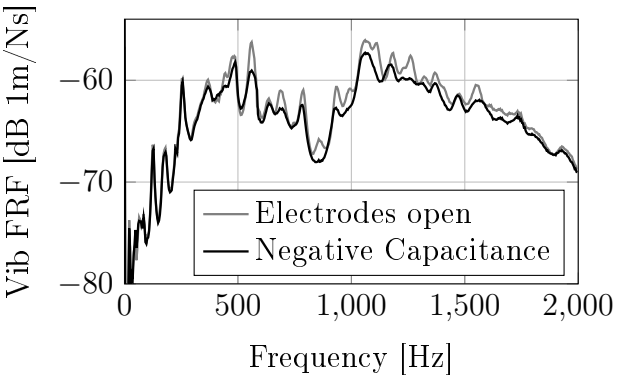

Figure 14: Vibration FRF of panel with open electrodes and negative capacitance

By that, two effects are visible in Figure 13. First the total passive damping of the panel appears to have rised, because the curve of the panel with PZT transducers lies under the FRF of the blank panel in most of the measured frequency range. Second, a shift of some eigenfrequencies is likely, when looking e.g. at the peak at 600 Hz or 1100 Hz, where the FRF seems to be shifted to lower frequencies. This indicates a dominance of the transducer mass over their stiffness at least at these frequencies.

With the piezoelectric transducers applied, the influence of negative capacitance damping can be measured. Therefore the vibration FRF are obtained with open electrodes at the transducers first and then with the negative capacitance circuits applied. In this case, a reference capacitance of $C_1 = 200\,\text{nF}$ is used. Figure 14 shows the results of this measurement.

Obviously, the damping effect of the negative capacitance circuit is much lower compared to the pretests at the steel panel. Below a frequency of 500 Hz, nearly no reduction of the vibration FRF is visible. Between 500 Hz and 1800 Hz resonances are damped by less than 3 dB. Above this frequency range, both curves appear to be nearly similar.

This fact becomes more obvious, if the vibration FRF of Figure 14 are summed to 3rd octave bands. In this visualization in Figure 15, a difference in the curves with and without negative capacitance circuits is hardly visible.

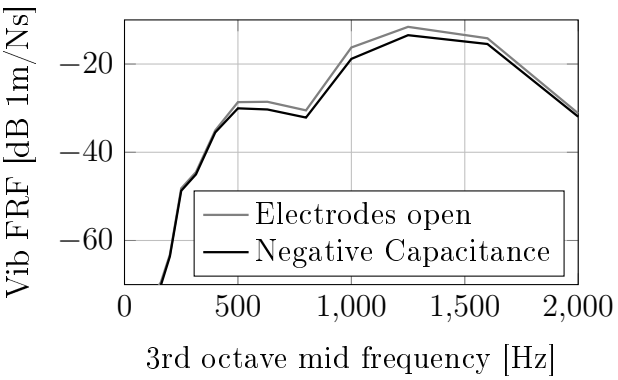

Figure 15: Vibration 3rd octave bands with and without negative capacitance

Therefore Figure 16 shows the difference between the two curves in Figure 15 to give a more detailed insight in the additional damping caused by the negative capacitance. It can be seen, that a small damping is present over the already mentioned frequency range, which reaches its maximum at the 3rd octave mid frequency of 1000 Hz with 2.58 dB. This is much less compared to the results presented in Figure 9, where 12.5 dB have been achieved in maximum.

Finally, the TL of the panel with and without negative capacitance circuit is investigated. Therefore the excitation is switched to an acoustic diffuse field, so that the incident sound power and the transmitted sound power

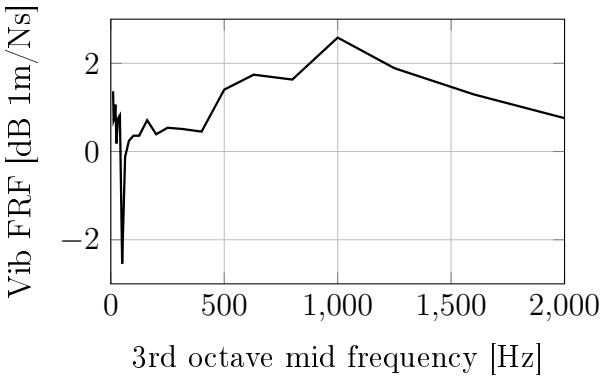

Figure 16: Difference of vibration amplitude in 3rd octave band with and without negative capacitance

can be estimated. With the mentioned test setup, the TL curves shown in Figure 17 in 3rd octave bands are obtained. Comparably to the results of the vibration amplitude reduction, the increase of the TL due to negative capacitance damping is nearly negligible. Only for frequencies above 4000 Hz the black curve indicating the damped TL is visible above the gray curve with open electrodes.

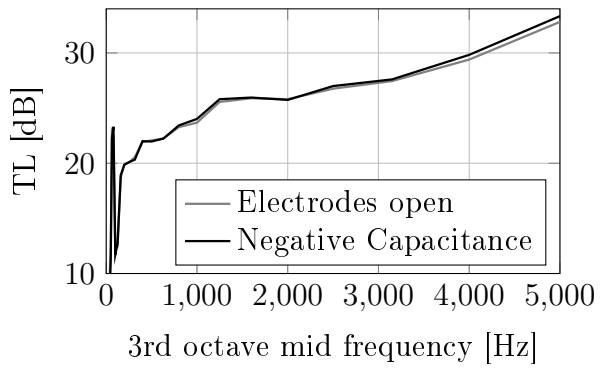

Figure 17: Difference of TL in 3rd octave band with and without negative capacitance

For a better visualization, the difference of both TL curves in Figure 17 is additionally plotted in Figure 18. There the maximum increase of the TL due to negative capacitance shunting can be seen at frequencies of 80 Hz and 2000 Hz with a value of ≈ 0.5 dB. This increase of the TL is even less than the amplitude reduction of the vibration FRF presented in Figure 16.

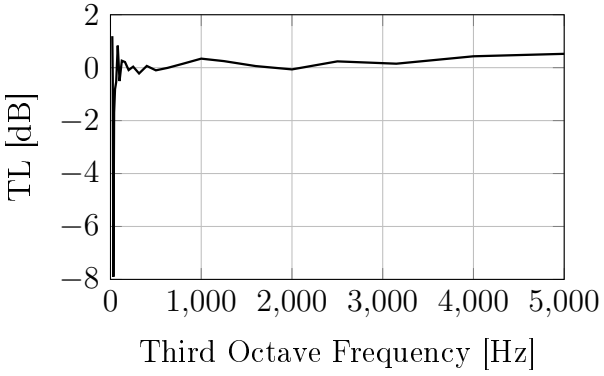

Figure 18: Difference of TL in 3rd octave band with and without negative capacitance

In fact, TL measurements with such low differences additionally comprise uncertainties caused by acoustic flanking transmissions in the test opening, noise and deviations due to the manual scanning of the surface with the sound intensity probe. These aspects have to be kept in mind when regarding the presented results. In conclusion, the effect of negative capacitance shunting of such sandwich panels seems to be negligible under the circumstances of the executed experiments.

5 DISCUSSION

In section 3 a steel panel has been investigated in terms of negative capacitance shunt damping. Due to promising results, this approach was transferred to a glass fiber sandwich helicopter trim panel. In both cases, the same amount of piezoelectric transducers has been used at the same negative capacitance circuits. If 10 or 20 individual negative capacitance networks are used is more or less insignificant, because the use of more individual circuits is even better for high frequencies with short wavelengths [12]. The only differences of the setups are by that their size and the material of the panels.

In fact, the sizes are 800×600 mm for the steel panel and 840×840 mm for the free section

of the sandwich panel outside the clamping at the edges. This yields in a surface factor of 1.47 between both panels. Therefore a reduced damping effect is expectable, because the vibration energy can spread over a wider area on the sandwich panel compared to the steel panel. If the same area of transducers is used, there is relatively less surface to access vibrations with the transducers for energy conversion and vibration damping.

In addition, the material and the setup of the panels appears to be the cause for the deviations in the effect of the negative capacitance. The differences between both panels are first the material. The first panel uses steel with a very high stiffness and density compared to the sandwich panel, which has glass fiber surface layers and a foam core. Therefore the relations of the stiffness between the actuator and the base material are different. Second the sandwich panel is much thicker compared to the only 2 mm thin steel sheet. Third, the passive structural damping seems to be higher for the sandwich panel compared to the steel panel, when looking at the Figure 8 and 13, because in the second figure, the resonances appear much softer and lower.

Bringing these facts together, it can be stated, that first the additional passive damping of the panel consumes much of the visual damping effect of the negative capacitance shunt since the achievable maximum combined damping will not be much greater. Second, due to the different stiffnesses of the sandwich and the steel panel, deviations in the coupling of the transducer to the structures are probable.

To investigate this further, a numerical finite element simulation is done, where both panels are excited by one piezoelectric transducer of 50×30 mm size. The amplitude of the resulting vibration FRF can be seen as measure for the coupling of the transducers. The higher it is, the more damping is expectable, if the negative capacitance circuit remains unchanged. Figure 19 shows the simulated FRF for an excitation of the panel with a single piezoelectric transducer in 3rd octave bands. As expected, the FRF of the steel panel shows a higher controllability with the actuator especially for low frequencies below 500 Hz.

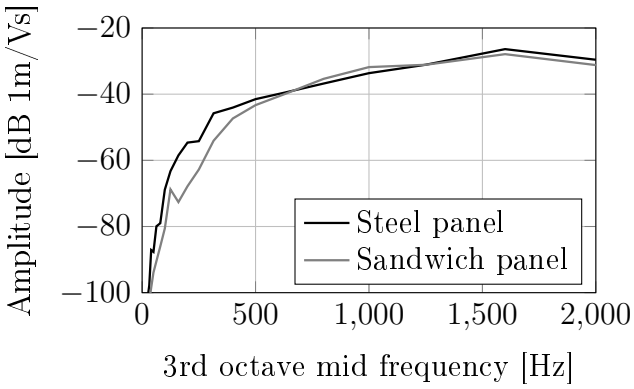

Figure 19: Simulated FRFs of excited steel and sandwich panel

This becomes more obvious, if the difference between both curves is plotted. In Figure 20 they are visualized, where the FRF of the sandwich panel is subtracted from the FRF of the steel panel. There it can be seen, that the difference between both panels in this case nearly reaches 15 dB in maximum. Because the piezoelectric coupling has a squared influence on negative capacitance damping [12], it is easy to see, that by this, the damping effect must be lower for the sandwich panel compared to the steel panel at low frequencies.

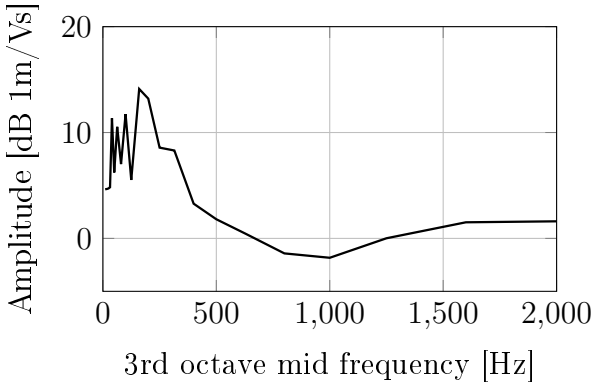

Figure 20: Difference of simulated FRFs of excited steel and sandwich panel

6 CONCLUSION AND OUTLOOK

In this paper, the applicability of piezoelectric shunt damping to improve the vibroacoustic characteristics of sandwich helicopter trim panels has been investigated. Therefore, preliminary tests of a multiple individual negative capacitance circuit damping systems have been performed on a steel panel. From these tests, a remarkable reduction of the structural vibration could be obtained.

Thereupon, a comparable system was transferred to a sandwich panel. For comparison, the same amount of transducers was used. Measurements of the vibration reduction as well as the improvement of the TL indicate a reduced damping effect of the negative capacitance compared to the steel panel. Based upon numerical simulations, it seems obvious, that a combination of the higher intrinsic damping of the sandwich panel and a much lower piezoelectric coupling of the transducers are responsible for this severe loss of function.

Therefore, the concept required some changes for future applications. The most important improvement is constituted by matching the piezoelectric transducer to the structural characteristics of the sandwich panel in order to increase the piezoelectric coupling. By this, the overall performance of the negative capacitance damping will be enlarged in the same manner. Second the influence of other transducer distributions, amounts and arrangements should be investigated besides the regular shape used for the tests in this paper.

References

[1] Fahy, F. J. and Gardonio, P., [*Sound and structural vibration: radiation, transmission and response*], Academic press (2007).

[2] Behrens, S., Fleming, A., and Moheimani, S., "A broadband controller for shunt piezoelectric damping of structural vibration," *Smart materials and structures* **12**, 18 (2003).

[3] Moheimani, S. R. and Fleming, A. J., "Piezoelectric shunt damping," *Piezoelectric Transducers for Vibration Control and Damping* , 73–91 (2006).

[4] De Marneffe, B. and Preumont, A., "Vibration damping with negative capacitance shunts: theory and experiment," *Smart Materials and Structures* **17**, 035015 (2008).

[5] Hagood, N. and von Flotow, A., "Damping of structural vibrations with piezoelectric materials and passive electrical networks," *Journal of Sound and Vibration* **146**(2), 243–268 (1991).

[6] Hollkamp, J., "Multimodal passive vibration suppression with piezoelectric materials and resonant shunts," *Journal of Intelligent Material Systems and Structures* **5**(1), 49–57 (1994).

[7] Behrens, S., Moheimani, S., and Fleming, A., "Multiple mode current flowing passive piezoelectric shunt controller," *Journal of Sound and Vibration* **266**(5), 929–942 (2003).

[8] Park, C. H. and Baz, A., "Vibration control of beams with negative capacitive shunting of interdigital electrode piezoceramics," *Journal of Vibration and Control* **11**(3), 331–346 (2005).

[9] Park, C. and Park, H., "Multiple-mode structural vibration control using negative capacitive shunt damping," *Journal of Mechanical Science and Technology* **17**(11), 1650–1658 (2003).

[10] Philbrick, G., [*Applications Manual for Computing Amplifiers for Modelling, Measuring, Manupulating & Much Else*], G. A. Philbrick Researches Inc. (1966).

[11] Pohl, M. and Rose, M., "Piezoelec-

tric shunt damping of a circular saw blade with autonomous power supply for noise and vibration reduction," *Journal of Sound and Vibration* **361**, 20–31 (2016).

[12] Pohl, M., *Elektromechanische Netzwerke mit adaptiven negativen Kapazitäten zur breitbandigen Schall- und Schwingungsreduktion*, PhD thesis, Technische Universität Carolo-Wilhelmina zu Braunschweig (2015).

[13] PI Ceramic GmbH, "DuraAct Piezoelectric Patch Transducers for Industry and Research," (2007). *available at* http://www.pi-portal.ws/index.php?option=com_docman&task=doc_download&gid=1050&Itemid=6 (*last reviewed* 2013/01/22).

[14] Texas Instruments Inc., "OPA445 High Voltage FET Input Operational Amplifier," (2008). *available at* http://www.ti.com/lit/ds/symlink/opa445.pdf (*last reviewed* 2013/01/22).